Investigation of the Electronic Structures of η-Cyclopentadienyl Transition-metal Dihalide Dimers†

Jennifer C. Green,* Malcolm L. H. Green, Philip Mountford, and Michael J. Parkington
Inorganic Chemistry Laboratory, South Parks Road, Oxford OX1 3QR

Extended-Hückel molecular-orbital calculations for the model systems $[W_2(cp)_2Cl_4]$, $[Mo_2(cp)_2(\mu\text{-}Cl)_4]$, and $[Re_2(cp)_2Cl_2(\mu\text{-}Cl)_2]$ (cp = $\eta\text{-}C_5H_5$) were used to analyse the bonding in the three observed, distinct geometries of metal–metal bonded (η-cyclopentadienyl)transition metal dihalide dimers of the general formula $[\{M(\eta\text{-}C_5R_5)X_2\}_2]$, and are supported by He I and He II photoelectron spectra for $[W_2(\eta\text{-}C_5H_4Pr^i)_2Cl_4]$ and by a He I photoelectron spectrum for $[Mo_2(\eta\text{-}C_5H_4Me)_2(\mu\text{-}Br)_4]$. The He I and He II photoelectron spectra are also reported for the related complex $[Mo_2(\eta\text{-}C_5H_4Pr^i)_2(\mu\text{-}SMe)_4]$. The calculations show that the metal *d*-electron count is the most important factor selecting the observed geometry of $[\{M(\eta\text{-}C_5R_5)X_2\}_2]$ (X = Cl or Br) species, but that the extent of metal–metal overlap and non-bonding interactions within the $(\mu\text{-}X)_4$ linkages of the quadruply bridged isomers must also be considered.

We have recently described the syntheses and dramatically different molecular structures of the congeneric pair of compounds $[W_2(\eta\text{-}C_5H_4Pr^i)_2Cl_4]$ (**1**)[1] and $[Mo_2(\eta\text{-}C_5H_4Pr^i)_2(\mu\text{-}Cl)_4]$ (**2**).[2] These compounds are members of a class of

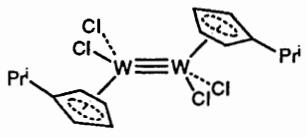

(1)

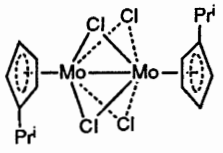

(2)

general formula $[\{M(\eta\text{-}C_5R_5)X_2\}_2]$ (X = halogen) examples of which are now known for M = Sc, Ti, V, Nb, Ta, Cr, Mo, W, Re, Ru, Co, Rh, or Ir. These compounds represent an important class of synthons within which three distinct structural types are encountered. These have been designated type (**I**), (**II**), or (**III**). The type (**I**) structure has each metal atom in a pseudo-tetrahedral co-ordination environment, and may or may not contain a metal–metal bond. Type (**II**) structures invariably possess a metal–metal bond and feature four bridging halide ligands and axially co-ordinated cyclopentadienyl ligands. Finally, the type (**III**) structure exists as a staggered, pseudo-

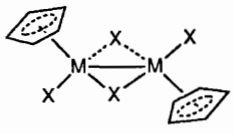

(I)

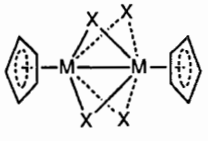

(II)

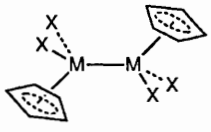

(III)

ethane-like dimer with no bridging halide ligands and a *trans* disposition of the two cyclopentadienyl rings.

Table 1. Crystallographically characterised $[\{M(\eta\text{-}C_5R_5)X_2\}_2]$ compounds

Compound	Type[a]	M–M[b]/Å	Ref.
$[W_2(\eta\text{-}C_5H_4Pr^i)_2Cl_4]$	(III)	2.367 8(8)	1
$[V_2(\eta\text{-}C_5Me_4Et)_2(\mu\text{-}Br)_4]$	(II)	2.565(1)	33
$[Ta_2(\eta\text{-}C_5Me_5)_2(\mu\text{-}Br)_4]$	(II)	2.748(2)	31
$[Mo_2(\eta\text{-}C_5H_4Pr^i)_2(\mu\text{-}Cl)_4]$	(II)	2.607(1)	2
$[Re_2(\eta\text{-}C_5H_4Et)_2Cl_2(\mu\text{-}Cl)_2]$	(I)	2.506(1)	8
$[Ru_2(\eta\text{-}C_5Me_5)_2Cl_2(\mu\text{-}Cl)_2]$	(I)	—	37
$[Cr_2(cp)_2Cl_2(\mu\text{-}Cl)_2]$	(I)	—	38
$[Cr_2(\eta\text{-}C_5Me_5)_2Cl_2(\mu\text{-}Cl_2)]$	(I)	—	*c*
$[Cr_2(\eta\text{-}C_5Me_5)_2Br_2(\mu\text{-}Br)_2]$	(I)	—	*d*
$[Rh_2(\eta\text{-}C_5Me_5)_2Cl_2(\mu\text{-}Cl)_2]$	(I)	—	*e*
$[Rh_2(\eta\text{-}C_5Me_5)_2Br_2(\mu\text{-}Br)_2]$	(I)	—	*f*
$[Rh_2(\eta\text{-}C_5Me_5)_2I_2(\mu\text{-}I)_2]$	(I)	—	*g*
$[Ir_2(\eta\text{-}C_5Me_5)_2Cl_2(\mu\text{-}Cl)_2]$	(I)	—	*h*
$[Ir_2(\eta\text{-}C_5Me_5)_2Br_2(\mu\text{-}Br)_2]$	(I)	—	*h*
$[Ir_2(\eta\text{-}C_5Me_5)_2Ir_2(\mu\text{-}I)_2]$	(I)	—	*h*

[a] See text for definition. [b] Only given for compounds in which a metal–metal bond exists. [c] F. H. Köhler, J. Lachmann, G. Müller, H. Zeh, H. Brunner, J. Pfauntsch, and J. Wachter, *J. Organomet. Chem.*, 1989, **365**, C15. [d] D. M. Morse, T. B. Rauchfuss, and S. R. Wilson, *J. Am. Chem. Soc.*, 1988, **110**, 8234. [e] M. R. Churchill, S. A. Julius, and F. J. Rotella, *Inorg. Chem.*, 1977, **16**, 1137. [f] M. R. Churchill and S. A. Julius, *Inorg. Chem.*, 1978, **17**, 3011. [g] M. R. Churchill and S. A. Julius, *Inorg. Chem.*, 1979, **18**, 2918. [h] M. R. Churchill and S. A. Julius, *Inorg. Chem.*, 1979, **18**, 1215.

Crystallographically characterised η-cyclopentadienyl transition-metal dihalide dimers are collected in Table 1. The actual structural type adopted by a compound $[\{M(\eta\text{-}C_5R_5)X_2\}_2]$ appears to depend most critically upon the identity of M. In order to test this hypothesis, and to gain a more thorough understanding of the bonding in the general class of compounds $[\{M(\eta\text{-}C_5R_5)X_2\}_2]$, a series of studies were undertaken employing the extended-Hückel computational technique[3] for the model compounds $[W_2(cp)_2Cl_4]$ [type (**III**)], $[Mo_2(cp)_2(\mu\text{-}Cl)_4]$ [type (**II**)], and $[Re_2(cp)_2Cl_2(\mu\text{-}Cl)_2]$ [type (**I**)] (cp = $\eta\text{-}C_5H_5$). The theoretical results were supplemented by gas-phase photoelectron (p.e.) spectroscopic studies of the real complexes

† *Non-S.I. unit employed:* eV ≈ 1.6 × 10^{-19} J.

Table 2. Structural parameters (distances in Å, angles in °) for the extended-Hückel calculations

	$[W_2(cp)_2Cl_4]$	$[Mo_2(cp)_2(\mu\text{-}Cl)_4]$	$[Re_2(cp)_2Cl_2(\mu\text{-}Cl)_2]$
M–M	2.368	2.61	2.50
M–Cl_t [a]	2.32	—	2.35
M–Cl_b [b]	—	2.48	2.40
M–Cp_{cent} [c]	2.06	2.00	2.06
C–C	1.41	1.41	1.41
C–H	1.04	1.04	1.04
M–M–Cp_{cent}	118.6	180.0	119.0
M–M–Cl_t	100.3	—	100.0
M–M–Cl_b	—	58.4	58.6
M–Cl_b–M	—	63.2	62.8

[a] Cl_t refers to the terminal chloride ligands. [b] Cl_b refers to the bridging chloride ligands. [c] Cp_{cent} refers to the η-C_5H_5 ring centroid; cp rings idealised to pentagons.

$[W_2(\eta\text{-}C_5H_4Pr^i)_2Cl_4]$[1] and $[Mo_2(\eta\text{-}C_5H_4Me)_2(\mu\text{-}Br)_4]$ (**3**).[4] The structural parameters used in the extended-Hückel calculations are listed in Table 2.

We also describe here He I and He II p.e. spectra of the related quadruply bridged μ-thiolato derivative $[Mo_2(\eta\text{-}C_5H_4Pr^i)_2(\mu\text{-}SMe)_4]$ (**4**),[5] which is closely related to the type (**II**) (quadruply bridged) tetrahalide analogues $[Mo_2(\eta\text{-}C_5H_4R)_2(\mu\text{-}X)_4]$ (X = Cl or Br). The electronic structure of the model complex $[Mo_2(cp)_2(\mu\text{-}SH)_4]$ has been investigated previously using extended-Hückel computational techniques.[6,7]

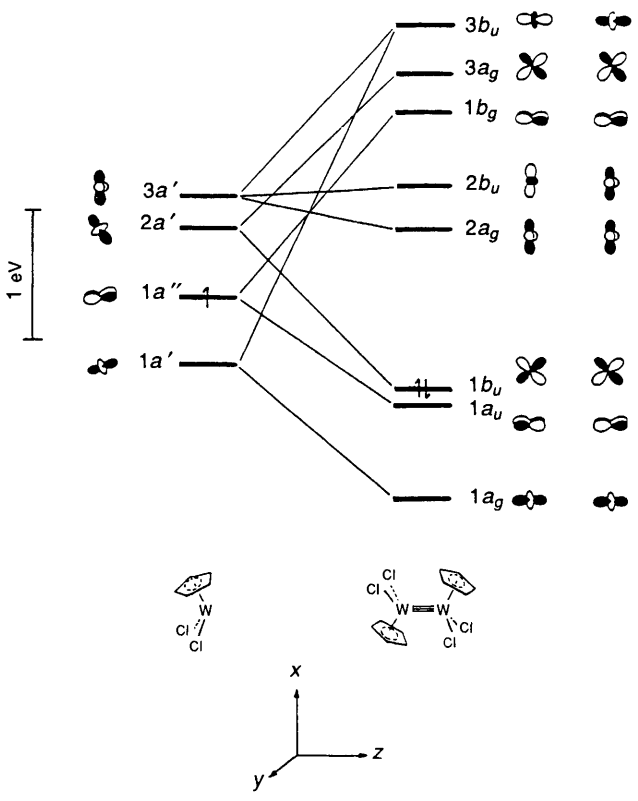

Figure 1. Interaction diagram for $[W_2(cp)_2Cl_4]$

Experimental

Samples of $[W_2(\eta\text{-}C_5H_4Pr^i)_2Cl_4]$[1] and $[Mo_2(\eta\text{-}C_5H_4Me)_2(\mu\text{-}Br)_4]$[4] were prepared as described previously. A sample of $[Mo_2(\eta\text{-}C_5H_4Pr^i)_2(\mu\text{-}SMe)_4]$[5] was provided by Dr. D. P. S. Rodgers of this laboratory.

The He I and He II p.e. spectra were obtained on a PES Laboratories model 0078 photoelectron spectrometer interfaced with a Research Machines 380Z microprocessor for data collection. The spectrometer consisted of a photon source, an ionisation chamber, and an electron analyser. The photon source was a Helectros Developments Ltd. helium discharge lamp and could generate both He I and He II radiation ($h\nu$ = 21.21 and 40.81 eV respectively). The lamp was also used to heat the samples. The analyser operates by electrostatic deflection of the electrons in a 127° cylindrical sector, across which the potential is varied to scan through the range of electron kinetic energies (k.e.s.). The electrons were detected by a Channeltron electron multiplier. Spectra were collected by repeated scans of about 54 s in order to minimise relative intensity changes of the bands due to temperature fluctuations. There was no apparent drift during data collection.

The three complexes (**1**), (**3**), and (**4**) were heated in order to obtain a sufficiently high count rate; $[W_2(\eta\text{-}C_5H_5Pr^i)_2Cl_4]$ and $[Mo_2(\eta\text{-}C_5H_4Pr^i)_2(\mu\text{-}SMe)_4]$ sublimed at a sufficient rate to collect both He I and He II photoelectron spectra, $[Mo_2(\eta\text{-}C_5H_4Me)_2(\mu\text{-}Br)_4]$ sublimed only slowly at 150 °C and decomposed at higher lamp temperatures. Therefore, only He I data could be obtained for the latter complex. The chloride-supported analogue, $[Mo_2(\eta\text{-}C_5H_4Pr^i)_2(\mu\text{-}Cl)_4]$, decomposed on attempted sublimation. All spectra were calibrated with reference to xenon, nitrogen, and the helium self-ionisation band [apparent ionisation energy (i.e.) = 4.99 eV].

The calculations were performed on the model systems $[W_2(cp)_2Cl_4]$ [structural type (**III**)], $[Mo_2(cp)_2(\mu\text{-}Cl)_4]$ [type (**II**)], and $[Re_2(cp)_2Cl_2(\mu\text{-}Cl)_2]$ [type (**I**)] using a modified extended-Hückel method employing weighted H_{ij} values.[3] The atomic co-ordinates were idealised to C_{2h} symmetry, but otherwise bond lengths and angles were taken from the crystal structures of $[W_2(\eta\text{-}C_5H_4Pr^i)_2Cl_4]$,[1] $[Mo_2(\eta\text{-}C_5H_4Pr^i)_2(\mu\text{-}Cl)_4]$,[2] and $[Re_2(\eta\text{-}C_5Me_4Et)_2Cl_2(\mu\text{-}Cl)_2]$.[8] The structural parameters used in this study are collected in Table 2. The atomic parameters for the extended-Hückel calculations were taken from previous work.[9]

Results and Discussion

Type (**III**) *Species: Extended-Hückel Molecular-orbital Study of* $[W_2(cp)_2Cl_4]$.—We begin our discussion with the type (**III**) structure in which the absence of bridging ligands yields a very straightforward interpretation of metal–metal and metal–ligand bonding. The molecular orbitals of the hypothetical type (**III**) species $[W_2(cp)_2Cl_4]$ are constructed from the fragment orbitals of two $W(cp)Cl_2$ units whose frontier orbitals are given at left in Figure 1. The orbitals of the related fragments $M(cp)(CO)_2$,[10] $Re(cp)H_2$,[11] and $Mo(cp)Cl_2$[12] have been discussed in detail previously. The result of allowing two $W(cp)Cl_2$ fragments to interact to give non-bridged, staggered $[W_2(cp)_2Cl_4]$ is shown at right in Figure 1.

The W–W bond of the composite molecule lies along the z axis, with the origin of the local co-ordinate system at its centre. For the C_{2h} point group, z is normally taken as the two-fold axis, but here y is chosen in order to maintain the normal choice of orbitals for metal–metal bonding.

Although the actual symmetry is much lower than cylindrical, the characterisation of metal-based orbitals according to the σ, π, and δ notation is nevertheless a useful distinction based on predominant orbital type, and gives an easy comparison with other metal–metal multiply bonded systems. The metal-based interactions separate out nicely into a σππδδ*π*π*σ* ordering, with the six metal electrons occupying one σ and two π orbitals. This affords a $(\sigma)^2(\pi)^4$ valence configuration, consistent with a

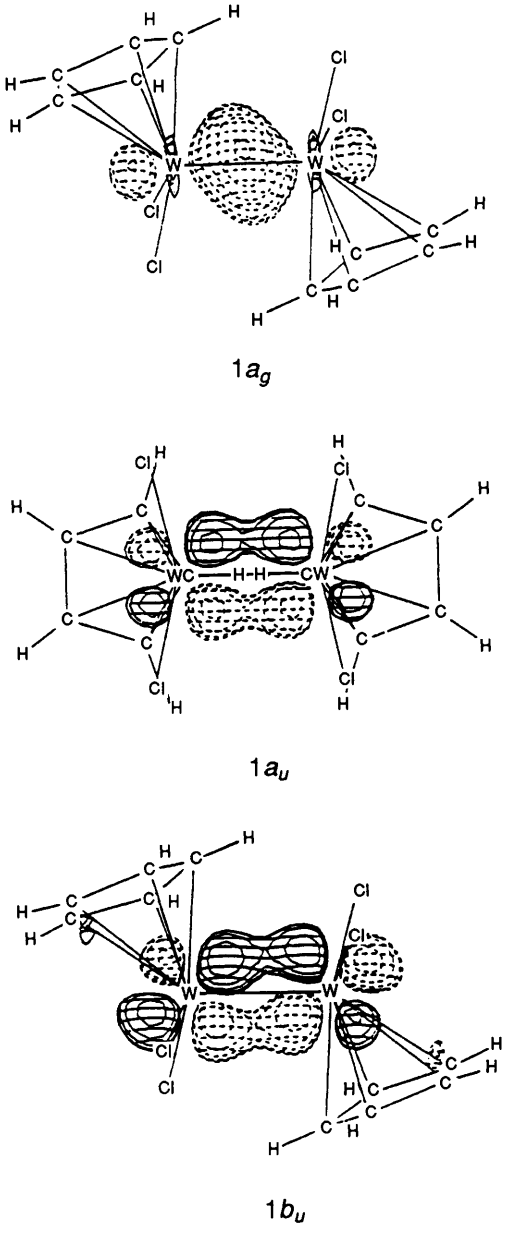

Figure 2. Contour diagrams of the $1a_g$, $1a_u$, and $1b_u$ orbital wavefunctions of $[W_2(cp)_2Cl_4]$

metal–metal triple bond for the present electron count. The two π levels ($1a_u$ and $1b_u$) are nearly isoenergetic (computed separation = 0.09 eV) and the σ level ($1a_g$) is calculated to be 0.74 eV below $1a_u$ based on the extended-Hückel method. The virtual δ and δ^* orbitals arise predominantly from the in- and out-of-phase combinations of the metal $5d_{x^2-y^2}$ atomic orbitals. The level ordering computed for $[W_2(cp)_2Cl_4]$ is virtually identical to that recently obtained by the Fenske-Hall method for the hypothetical isostructural complex $[Re_2(cp)_2H_4]$,[11] consistent with the view that Cl is a relatively poor π-donor ligand.

The three highest-occupied molecular orbitals (h.o.m.o.s) ($1b_u$, $1a_u$, and $1a_g$) are predominantly metal-based and are calculated to have 88, 82, and 77% tungsten character respectively. The two lowest-unoccupied molecular orbitals (l.u.m.o.s) are also metal-based and have 74 ($2a_g$) and 82% ($2b_u$) tungsten character. Contour diagrams of the σ ($1a_g$), $\pi(yz)(1a_u)$, and $\pi(xz)(1b_u)$ orbital wavefunctions of $[W_2(cp)Cl_4]$ that make up the metal–metal bonding manifold are shown in Figure 2.

The electronic structure of $[W_2(cp)_2Cl_4]$ may be compared to those of the related $[M_2L_6]$ (M = Mo or W; L = R, OR, or NR_2) d^3–d^3 dimers.* These complexes also have a metal–metal triple bond with a valence electronic configuration $(\sigma)^2(\pi)^4$ as confirmed by p.e. studies [13,14] and a variety of molecular-orbital calculations. Xα-SW calculations [13] have been performed on $[Mo_2(OH)_6]$, $[Mo_2(NH_2)_6]$, $[Mo_2(NMe_2)_6]$, and $[Mo_2Me_6]$, and agree well with the results of p.e. studies. For L = Me or OH the h.o.m.o. is a metal–metal π-bonding orbital of e_u symmetry (in the D_{3d} point group), but for L = NH_2 or NMe_2 the h.o.m.o. is a nitrogen lone pair of either a_{2g} or a_{1u} symmetry with the $(\sigma)^2(\pi)^4$ manifold lower in energy. For L = alkyl, extensive mixing is observed between M–M and M–C bonding orbitals which complicates the simple description of the valence electronic structure as $(\sigma)^2(\pi)^4$.

The l.u.m.o. in each of these four complexes was calculated to be a Mo–Mo π^* orbital of e_g symmetry as opposed to the δ-type orbital found in this study for $[W_2(cp)_2Cl_4]$. The differences for the other $[M_2L_6]$ compounds arise from better L→M π donation, and from the higher symmetry (D_{3d}) which permits extensive π–δ mixing. Even in $[Mo_2Me_6]$ where there is no L→M π donation the e_u orbital (h.o.m.o.), while predominantly Mo–Mo π bonding, also has substantial δ^* character due to mixing allowed by the C_3 axis. For $[W_2(cp)_2Cl_4]$, however, our calculations find little mixing between either the $\pi(xy)$ and $\delta^*(x^2 - y^2)$ combinations, or between the $\pi^*(xz)$ and $\delta(x^2 - y^2)$ combinations, although, by symmetry, mixing is allowed. For each of the complexes $[Mo_2L_6]$ (L = alkyl, alkoxide, or dialkylamide), the lowest-energy electronic transition occurs in the u.v. region and tails into the visible region of the spectrum, accounting for their characteristic yellow to red colours.[15] Our calculations for $[W_2(cp)_2Cl_4]$ indicate that lower-energy $\pi \longrightarrow \delta/\delta^*$ transitions are accessible in this system and may account for the green colour observed for the real complexes $[W_2(\eta\text{-}C_5H_4R)_2X_4]$ (X = Cl or Br). These features will be addressed in more detail later in this paper.

Photoelectron Spectroscopic Study of $[W_2(\eta\text{-}C_5H_4Pr^i)_2Cl_4]$. —The low-ionisation-energy regions of the He I and He II p.e. spectra of the representative type (**III**) species, (**1**), are shown in Figure 3, and the ionisation energies and assignments are presented in Table 3. The spectra comprise four groups of bands which have been designated A—D. The bands B, C, and D are assigned to ionisations arising from η-$C_5H_4Pr^i(\pi)$-, W–Cl(π)-, and W–Cl(σ)-based orbitals respectively, based on the p.e. spectra of other cyclopentadienyl metal halide systems.[16]. The marked increase in intensity of band A on passing from He I to He II ionising radiation is indicative of substantial metal *d* character in the orbitals out of which ionisation has occurred. The energy separation between bands A and B is *ca.* 2 eV.

Table 4 compares the important p.e. data for compound (**1**) with those obtained for some other $[M_2L_6]$ dimers of the $(\sigma)^2(\pi)^4$ configuration. For the alkoxide series, the σ- and π-ionisations are well resolved, but for $[Mo_2(NMe_2)_6]$ they were found to lie under one broad and asymmetric band. Moreover, for the $[M_2(OR)_6]$ series listed in Table 4 the bandwidths of the σ-based ionisations are quite narrow compared to those of the π-based ionisations. Intuitively, one would like to anticipate a stronger σ-bonding interaction (as indicated by orbital stability and bandwidth) than a π-bonding interaction.

* In this paper we will adopt the usual d^n–d^n-notation where 'n' refers to the number of metal valence *d* electrons in the ML_x fragments not employed in metal–ligand bonding.

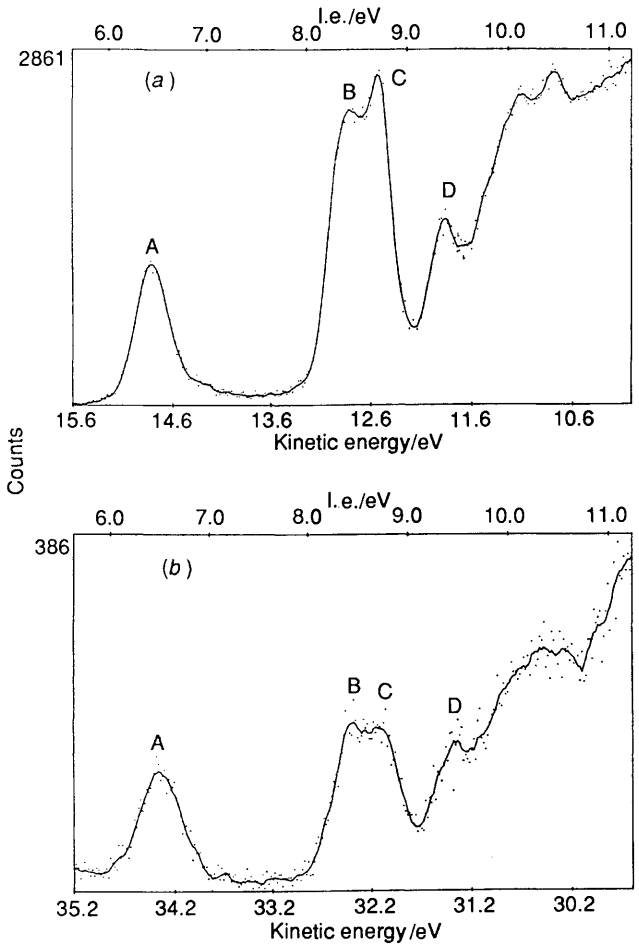

Figure 3. He I (*a*) and He II (*b*) p.e. spectra of $[W_2(\eta\text{-}C_5H_4Pr^i)_2Cl_4]$

Table 3. Assignment of the low-ionisation-energy region of the p.e. spectra of $[W_2(\eta\text{-}C_5H_4Pr^i)_2Cl_4]$ (**1**)

Band	I.e./eV	Assignment	Positive-ion state
A	6.48	$\sigma + \pi$	$^2A_g + (^2A_u, ^2B_u)$
B	8.54	$\eta\text{-}C_5H_4Pr^i(\pi)$	*
C	8.83	W–Cl(π)	*
D	9.38	W–Cl(σ)	*

* Composite band.

Table 4. Comparison of peak maxima and widths for metal ionisations of selected $[M_2L_6]$ complexes featuring a $(\sigma)^2(\pi)^4$ electronic configuration

	Maxima[a]/eV		
Complex	π	σ	Ref.
$[Mo_2(OCH_2Bu^t)_6]$	7.40[b]	8.02[b]	14
$[Mo_2(OPr^i)_6]$	7.33(0.69)	7.99(0.35)	21
$[Mo_2(OCH_2Bu^t)_6]$	7.46(0.69)	8.08(0.36)	21
$[Mo_2(OBu^t)_6]$	6.79(0.74)	7.80(0.43)	21
$[W_2(OBu^t)_6]$	6.27(0.82)	7.79(0.40)	21
$[Mo_2(NMe_2)_6]$	7.98[b,c]		14
$[W_2(\eta\text{-}C_5H_4Pr^i)_2Cl_4]$	6.48(0.41)[c]		*d*

[a] Full width at half-maximum in parentheses. [b] Peak width not available. [c] σ and π ionisations not resolved. [d] This work.

Similar phenomena have been noted in the p.e. spectra of quadruply bonded W_2 dimers.[17–19] P.e. spectroscopic data[20] for the quadruply bonded dimolybdenum species $[Mo_2(O_2CBu^t)_4]$ suggest that the σ and π ionisations are isoenergetic. The origin of this implied destabilisation of the σ level is thought to lie[21] in the close contact of the two metal atoms in a complex with an unsupported metal–metal bond. The close approach causes a substantial overlap, and consequently a repulsive interaction, between the valence nd_{z^2} orbitals of one metal atom and the outer core ns and np_z orbitals of the other. Thus the valence σ level is destabilised and its ionisation occurs at a similar energy to that for the π-based ionisations. Removal of an electron from this level reduces the valence repulsions with the outer core so bond-distance changes are relatively small; the metal–metal distance does not increase as one would normally expect for removing an electron from a σ-bonding orbital, and so a relatively narrow bandwidth is observed.

Where should one place the σ ionisation in compound (**1**)? From the above discussion it might be argued that band A contains both the π- and σ-based ionisations, and that there would otherwise be an unprecedented energy separation of >2 eV if the σ ionisation was placed under the next possible band (B). Moreover, this latter band does not exhibit any obvious metal *d* character based on the differences between the He I and He II p.e. spectra. However, one feature of band A is its symmetry and relatively narrow width, an observation which might militate against this band containing all three metal-based ionisations. Although the arguments outlined in the preceding paragraph for placing the σ ionisation higher, rather than lower, in energy might be diminished in this system owing to the larger metal–metal separation and anticipated *d*-orbital contraction, such changes would also reduce the extent of valence orbital–valence orbital overlap. In the absence of any compelling direct evidence to the contrary, it is most reasonable in the light of current understanding of metal–metal multiple bonding to assume that the σ ionisation in (**1**) lies under band A along with the π ionisations, analogous to that proposed for $[Mo_2(O_2CR)_4]$ systems.[20]

The width of the metal-based ionisations of compound (**1**) is narrow compared to those of the other $[M_2L_6]$ complexes listed in Table 4, suggesting that bond-distance changes occurring on removal of an electron from these orbitals are relatively small, a conclusion that is consistent with the anticipated *d*-orbital contraction and the relatively long W≡W bond length in this complex. Note, however, that for the $[M_2L_6]$ (D_{3d} symmetry) dimers the π ionisation also contains broadening due to spin–orbit splitting of the ^2E_u ion state ($\lambda_{Mo} \approx 0.1$, $\lambda_W \approx 0.2$—0.3 eV).[21] For (**1**), the anticipated positive-ion states are ^2A_g, ^2B_u, and ^2A_u for removing an electron from the σ, $\pi(xz)$, and $\pi(yz)$ orbitals respectively. In the C_{2h} triply bonded dimers $[M_2(CH_2Bu^t)_2(O_2CR)_4]$ (M = W, R = CF_3; M = Mo, R = Bu^t) the π ionisations (giving rise to isoenergetic ^2B_u and ^2A_u states) have bandwidths of 0.65 (M = W) and 0.54 eV (M = Mo) respectively.[19]

The p.e. data for $[W_2(\eta\text{-}C_5H_4Pr^i)_2Cl_4]$ suggest that this compound is almost as 'electron-rich' (as judged from the first i.e.) as $[W_2(OBu^t)_6]$, and even more so than any of the dimolybdenum alkoxide species listed in Table 4. Comparison may also be made with the related triply bonded tetracarbonyl derivatives $[M_2(cp)_2(CO)_4]$ for which first i.e.s of 7.25 (M = Cr), 7.35 (Mo), and 7.36 eV (W) have been reported.[22] The computational and p.e. spectroscopic results presented here are consistent with the observed chemical reactivity[1,23] of the W≡W triple bond in $[W_2(\eta\text{-}C_5H_4R)_2Cl_4]$, which is analogous to that of some other metal–metal triply bonded dimers.

Visible Spectra of $[W_2(\eta\text{-}C_5H_4R)_2Cl_4]$ (R = Me *or* Pr^i).—These green compounds show several overlapping absorptions

Table 5. Dipole-allowed low-energy transitions for $[W_2(\eta\text{-}C_5H_4R)_2Cl_4]$

Transition	Excited state
$\sigma \longrightarrow \delta^*(x^2 - y^2)$	^1B_u
$\pi(yz) \longrightarrow \delta(x^2 - y^2)$	^1A_u
$\pi(xz) \longrightarrow \delta(x^2 - y^2)$	^1B_u

in their visible spectra,[1] the intensities of which are consistent with metal *d–d* transitions. The extended-Hückel calculations for $[W_2(cp)_2Cl_4]$ reveal a pair of low-lying unoccupied molecular orbitals of δ and δ* symmetry with a relatively small computed separation (0.34 eV), placed *ca.* 1.3 eV above the π manifold. Recalling that the p.e. data for compound (**1**) suggested that the σ ($1a_g$) and π ($1b_u$ and $1a_u$) levels lie very close in energy, three dipole-allowed transitions might be anticipated. These are listed in Table 5 with all transitions arising from the ^1A_g ground state.

In the other $[M_2L_6]$ systems discussed above the molecular D_{3d} symmetry permits π–δ mixing which, together with substantial ligand-to-metal π donation, results in the removal of δ/δ* orbitals from the frontier region. Thus the lowest-energy transition in the species $[M_2L_6]$ (M = Mo or W; L = CH_2Bu^t, OBu^t, or NMe_2) lies in the u.v. region of the spectrum and was assigned as being the $\pi \longrightarrow \pi^*$ transition.[15] For the type (**III**) complexes $[W_2(\eta\text{-}C_5H_4R)_2Cl_4]$ the π–δ mixing is negligible and the poor π-donor ability of chloride and bromide results in the δ/δ* levels not being substantially destabilised by ligand-to-metal π donation. Interestingly, the related complex $[W_2(cp)_2(NMe_2)_4]$ is pale orange-yellow.[24] Since nitrogen (in NR_2) is a good π donor, these qualitative observations suggest that π donation from the dimethylamide ligands pushes the δ and δ* levels up in energy, removing the transitions listed in Table 5 from the visible region of the spectrum.

Type (**II**) *Species: Extended-Hückel Molecular-orbital Study of* $[Mo_2(cp)_2(\mu\text{-}Cl)_4]$.—We now consider the electronic structure of the quadruply bridged type (**II**) species $(M_2(\eta\text{-}C_5R_5)_2(\mu\text{-}X)_4]$. The model employed here is based on the structurally characterised homologue $[Mo_2(\eta\text{-}C_5H_4Pr^i)_2(\mu\text{-}Cl)_4]$[2] idealised to C_{2h} symmetry. Molecular-orbital descriptions of the related species $[Mo_2(cp)_2(\mu\text{-}SH)_4]$ and $[Mo_2(cp)_2(\mu\text{-}S)_4]$ have been given in detail previously.[6,7,25] In reality, d^1–d^1 tetra-μ-sulphido dimers are unknown, prefering to exist as the doubly bridged isomer *trans*-$[Mo_2(\eta\text{-}C_5R_5)_2S_2(\mu\text{-}S)_2]$.[26] Extended-Hückel molecular-orbital procedures have been used previously to examine the changes in frontier-level ordering upon co-ordination of H to the μ-S ligands of $[Mo_2(cp)_2(\mu\text{-}S)_4]$ to give first $[Mo_2(cp)_2(\mu\text{-}S)_2(\mu\text{-}SH)_2]$ (d^2–d^2), and then $[Mo_2(cp)_2(\mu\text{-}SH)_4]$ (d^3–d^3).[6,7]

The molecular orbitals of the hypothetical type (**II**) complex $[Mo_2(cp)_2(\mu\text{-}Cl)_4]$ may be constructed from the fragment orbitals of $Mo_2(cp)_2$ (given at left in Figure 4) and of $(\mu\text{-}Cl)_4$ (given at right in Figure 4). A detailed discussion of the derivation of the frontier molecular orbitals of $Mo_2(cp)_2$ has recently been given by Hoffmann and co-workers.[7] The eleven metal-based orbitals of $Mo_2(cp)_2$ transform as $4a_g + 2a_u + 2b_g + 3b_u$ under the C_{2h} symmetry of the final complex. The π(*xz*) and π(*yz*) orbitals are raised above the σ, δ, and δ* combinations since the former are derived from metal–ring antibonding orbitals of the Mo(cp) fragments.[27] The twelve 3*p* atomic orbitals of $(\mu\text{-}Cl)_4$ transform as $3a_g + 2a_u + 3b_g + 4b_u$ under C_{2h} symmetry. Thus, by symmetry, one metal-based orbital (a_g) and two ligand-based orbitals (one b_g and one b_u) should be left without partners and remain Mo–Cl non-bonding.

The result of allowing the two fragments to interact to give $[Mo_2(cp)_2(\mu\text{-}Cl)_4]$ is shown at the centre in Figure 4. The metal–

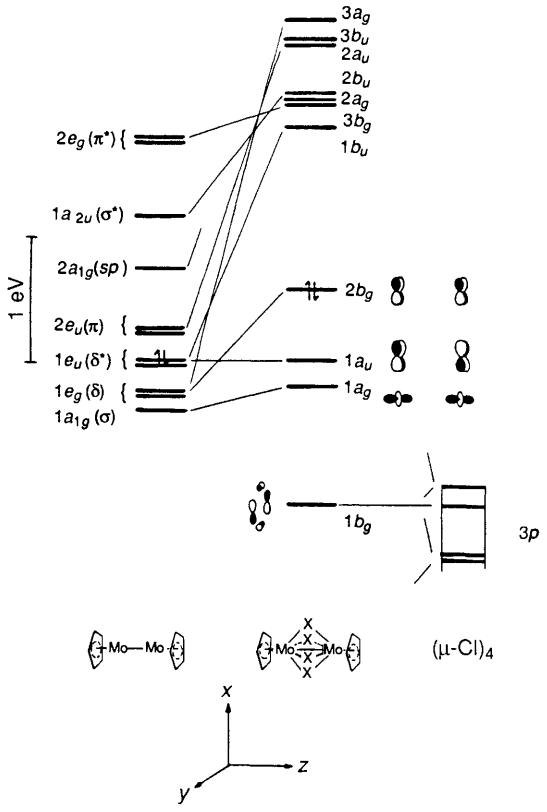

Figure 4. Interaction diagram for $[Mo_2(cp)_2(\mu\text{-}Cl)_4]$

metal bond lies along the *z* axis with the origin of the local co-ordinate system at its centre. The four chloride ligands lie at equal distances from the origin along the *x* and *y* axes.

In the composite molecule $[Mo_2(cp)_2(\mu\text{-}Cl)_4]$ the major effect of the four bridging ligands is to reduce the number and degeneracy of the metal-based frontier orbitals. The π, π*, $\delta(x^2 - y^2)$, and $\delta^*(x^2 - y^2)$ orbitals of the fragment $Mo_2(cp)_2$ are pushed high up in energy through strong interactions with the $(\mu\text{-}Cl)_4$ fragment. The introduction of the four bridging ligands effectively removes any Mo–Mo π-bonding interactions.

The three remaining metal-based orbitals, σ ($1a_g$), δ*(*xy*) ($1a_u$), and δ(*xy*) ($2b_g$), can accommodate up to six metal electrons. For the electron count under consideration here a $(\sigma)^2(\delta^*)^2(\delta)^2$ valence electronic configuration consistent with a Mo–Mo single bond results. Close to the $1a_g$ level is a ligand-based orbital ($1b_g$) which is a chlorine-based lone pair that does not find a suitable bonding combination with the $Mo_2(cp)_2$ fragment. Contour diagrams of the $(\mu\text{-}Cl)_4$ lone pair ($1b_g$), σ($1a_g$), δ*(*xy*) ($1a_u$), and δ(*xy*) ($2b_g$) orbital wavefunctions of $[Mo_2(cp)_2(\mu\text{-}Cl)_4]$ are shown in Figure 5.

An interesting feature of the level ordering in this complex is the reversal of the metal-based δ(*xy*) and δ*(*xy*) levels such that the antibonding combination lies below the bonding combination in energy. This reversal may be understood by considering the interactions between the δ(*xy*) and δ*(*xy*) orbitals of the $Mo_2(cp)_2$ fragment and the appropriate symmetry-adapted 3*p* atomic orbital combinations of the $(\mu\text{-}Cl)_4$ fragment as shown in Figure 6. In the $Mo_2(cp)_2$ fragment the two metal orbitals lie relatively close together in energy at the metal–metal separation used. The δ(*xy*) orbital finds a suitable match with the $(\mu\text{-}Cl)_4$ fragment whereas the δ*(*xy*) level does not. If the δ(*xy*)–$(\mu\text{-}Cl)_4$ interaction is large enough then the *metal-based* level ordering will be reversed to δ*(*xy*) lying below δ(*xy*). Such a situation is anticipated by the calculations presented here for $[Mo_2(cp)_2(\mu\text{-}Cl)_4]$, and a similar reversal was found for the

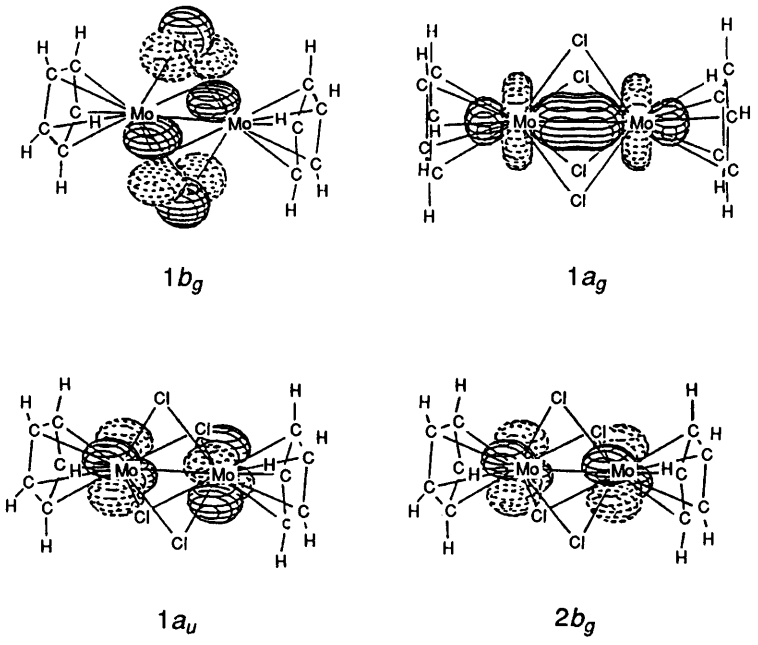

Figure 5. Contour diagrams of the $1b_g$, $1a_g$, $1a_u$, and $2b_g$ orbital wavefunctions of $[Mo_2(cp)_2(\mu\text{-}Cl)_4]$

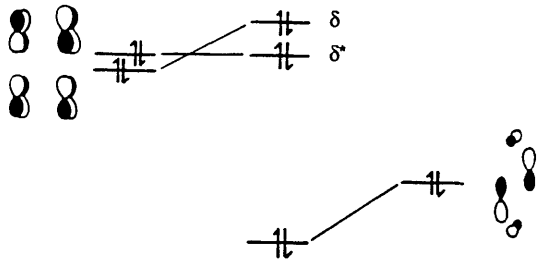

Figure 6. Illustration of the $(\mu\text{-}Cl)_4$–$\delta(xy)$ interaction in $[Mo_2(cp)_2(\mu\text{-}Cl)_4]$

related complexes $[Mo_2(cp)_2(\mu\text{-}S)_4]$ and $[Mo_2(cp)_2(\mu\text{-}SH)_4]$ using extended-Hückel calculations.[6,7]

Although the final level ordering cannot accurately be predicted from our calculations alone, a detailed structural study by Cotton and co-workers[28] of the isostructural series of edge-shared bioctahedral complexes $[M_2Cl_4(\mu\text{-}Cl)_2(dmpm)_2]$ [M = Ta, W, or Re; dmpm = bis(dimethylphosphino)methane] mitigates in favour of a $\delta^*(xy) < \delta(xy)$ ordering since *two* bridging ligands have the effect of achieving the same level reversal in the dmpm complexes, and the type (**II**) compounds under study here have *four* bridging halide ligands. The consequences of this reversal in level ordering are only important for d^2–d^2 $[M_2(\eta\text{-}C_5R_5)_2(\mu\text{-}X)_4]$ species (M = Group 5 metal) where, instead of a metal–metal double bond a formal bond order of $\leqslant 1$ is anticipated. A further implication of a $\sigma < \delta^* < \delta$ level ordering for a d^2–d^2 dimer is that the h.o.m.o. (δ^*) would be relatively high in energy, and at best metal–metal non-bonding. Such a level ordering readily accounts for some of the reactivity patterns of $[Ta_2(\eta\text{-}C_5Me_4R)_2(\mu\text{-}X)_4]$.[29] The complex $[Ta_2(\eta\text{-}C_5Me_5)(\mu\text{-}Br)_4]$ is reported to show a low-energy transition ($\lambda_{max.}$ = 794 nm, ε = 2 925 dm^3 mol^{-1} cm^{-1}) in its visible spectrum. From the results presented above the lowest-energy absorption for a type (**II**) dimer should represent the dipole-allowed $\delta^* \longrightarrow \delta$ ($^1A_g \longrightarrow {}^1B_u$) transition [note that the transition $\sigma \longrightarrow \delta$ ($^1A_g \longrightarrow {}^1B_g$) is dipole-forbidden].

Returning again to Figure 4, it is noted that the calculations reveal a small energy separation (0.2 eV) between the $1a_g$ (σ) and $1a_u$ (δ^*) levels, and a somewhat larger separation (0.56 eV) between $1a_u$ (δ^*) and $2b_g$ (δ). A similar pattern was found previously for $[Mo_2(cp)_2(\mu\text{-}S)_4]$ using extended-Hückel calculations. On passing from $[Mo_2(cp)_2(\mu\text{-}S)_4]$ to $[Mo_2(cp)_2(\mu\text{-}SH)_4]$, however, the δ/δ^* separation was found to decrease, and the $(\mu\text{-}X)_4$ lone pair (corresponding to $1b_g$ in Figure 4) dropped in energy. Earlier workers[6] used a small computed $1a_g/1a_u$ separation (< 0.10 eV) for $[Mo_2(cp)_2(\mu\text{-}S)_4]$ to account for the observation that structures of the type $[Mo_2(\eta\text{-}C_5R_5)_2(\mu\text{-}S)_4]$ are unknown, but that dimers of the type $[Mo_2(\eta\text{-}C_5R_5)_2(\mu\text{-}S)_2(\mu\text{-}SR')_2]$ and $[Mo_2(\eta\text{-}C_5R_5)_2(\mu\text{-}SR')_4]$ are quite stable. They suggested that, for a small $1a_g/1a_u$ separation and a d^1–d^1 electron count a paramagnetic complex or a second-order Jahn–Teller distortion might be anticipated for a quadruply bridged dimer.

More recently, Fenske-Hall molecular-orbital calculations for $[Mo_2(cp)_2(\mu\text{-}S)_4]$ gave a $(\sigma)^2\delta^*(xy)^2$ description of the metal-based orbitals, with a vacant sulphur-based orbital (corresponding to $1b_g$ in Figure 4) as the l.u.m.o. (h.o.m.o. – l.u.m.o. separation *ca.* 1.2 eV).[25] In these studies it was postulated that large S ··· S non-bonding interactions in the $(\mu\text{-}S)_4$ bridge (rather than a small computed h.o.m.o. – l.u.m.o. gap) were responsible for the preference of a doubly- rather than a quadruply-bridged geometry. The occurrence of quadruply bridged species $[Mo_2(\eta\text{-}C_5R_5)_2(\mu\text{-}S)_2(\mu\text{-}SR')_2]$ and $[Mo_2(\eta\text{-}C_5R_5)_2(\mu\text{-}SR')_4]$ was then considered to be consistent with such an analysis since co-ordination of alkyl groups to the μ-S ligands would lower lone pair–lone pair interactions inherent within the naked μ-sulphido bridges.

In an attempt to clarify the level ordering and its interpretation for dimers of the type $[M_2(\eta\text{-}C_5R_5)_2(\mu\text{-}X)_4]$ (X = halide, sulphide, or thiolate) p.e. spectroscopic studies of $[Mo_2(\eta\text{-}C_5H_4Me)_2(\mu\text{-}Br)_4]$ (**3**) and $[Mo_2(\eta\text{-}C_5H_4Pr^i)_2(\mu\text{-}SMe)_4]$ (**4**) were carried out.

Photoelectron Spectroscopic Study of $[Mo_2(\eta\text{-}C_5H_4Me)_2(\mu\text{-}Br)_4]$ *and* $[Mo_2(\eta\text{-}C_5H_4Pr^i)_2(\mu\text{-}SMe)_4]$.—The compound $[Mo_2(\eta\text{-}C_5H_4Me)_2(\mu\text{-}Br)_4]$ sublimes only slowly and a spectrum using He II ionising radiation could not be obtained. The tetrachloro-bridged species $[Mo_2(\eta\text{-}C_5H_4Pr^i)_2(\mu\text{-}Cl)_4]$ decomposed rapidly on attempted sublimation. The low-ionisation-potential region of the He I spectrum is shown in Figure

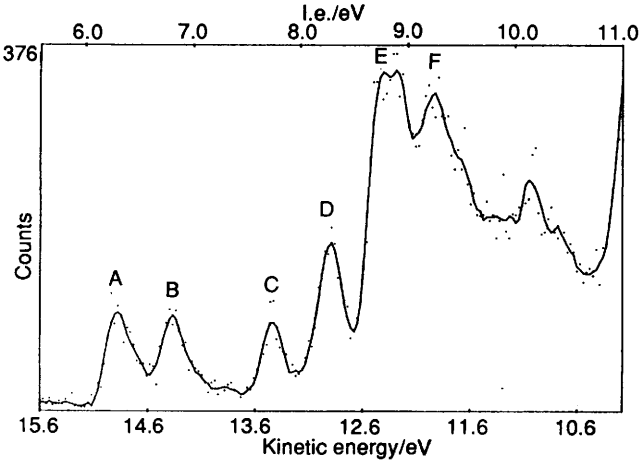

Figure 7. He I p.e. spectrum of $[Mo_2(\eta\text{-}C_5H_4Me)_2(\mu\text{-}Br)_4]$

Table 6. Assignment of the low-ionisation-energy region of the He I p.e. spectrum of $[Mo_2(\eta\text{-}C_5H_4Me)_2(\mu\text{-}Br)_4]$ (**3**)

Band	I.e./eV	Assignment	Positive-ion state[a]
A	6.29	$\delta(xy)$	^2B_g
B	6.79	$\delta^*(xy)$	^2A_u
C	7.78	σ	^2A_g
D	8.38	$(\mu\text{-Br})_4$ lone pair	^2B_g
E	8.92	$\eta\text{-}C_5H_4Me(\pi)$	*b*
F	9.43	Mo–Br	*b*

[a] Ion states for the local C_{4h} symmetry. [b] Composite band.

Table 7. Assignment of the low-ionisation-energy region of the He I and He II p.e. spectra of $[Mo_2(\eta\text{-}C_5H_4Pr^i)_2(\mu\text{-}SMe)_4]$ (**4**)

Band	I.e./eV	Assignment	Positive-ion state[a]
A	5.70	$\delta(xy)$	^2B_g
B	5.90	$\delta(xy)^*$	^2B_u
C	6.83	σ	^2A_g
D	7.84	$(\mu\text{-SMe})_4$ lone pair	*b*
E	8.23	Mo–SMe	*b*
F	8.66	$\eta\text{-}C_5H_4Pr^i(\pi)$	*b*
G	9.34	Mo–SMe	*b*

[a] Ion states for the local C_{4h} symmetry. [b] Composite band.

7, with the bands of interest labelled A—F. Assignments for the p.e. spectrum of compound (**3**) are given in Table 6, and are made assuming Koopmans' theorem[30] and the level ordering computed above for $[Mo_2(cp)_2(\mu\text{-}Cl)_4]$. As a check, the orbitals of $[Mo_2(cp)_2(\mu\text{-}Br)_4]$ were computed using structural parameters published previously for $[Ta_2(\eta\text{-}C_5Me_5)_2(\mu\text{-}Br)_4]$.[31] The frontier-level ordering was identical and gave very similar relative energies to those computed for $[Mo_2(cp)_2(\mu\text{-}Cl)_4]$.

In the absence of a He II p.e. spectrum, the degree of metal character of the orbitals associated with the four low-ionisation-energy bands A—D cannot be assessed. It is noteworthy though that the three bands of lowest i.e. (A—C) all have similar intensities. This is to be expected since the orbitals from which they are thought to arise have similar localisation properties and so the band intensities should, to a first approximation, be proportional only to orbital occupancy.[32]

In contrast to its relatively involatile tetrabromide analogue, the μ-thiolato species, (**4**), sublimed readily and the low-ionisation-energy regions of its He I and He II p.e. spectra are shown in Figure 8. The bands of interest here are labelled A—G, and their assignments are given in Table 7. The marked increase

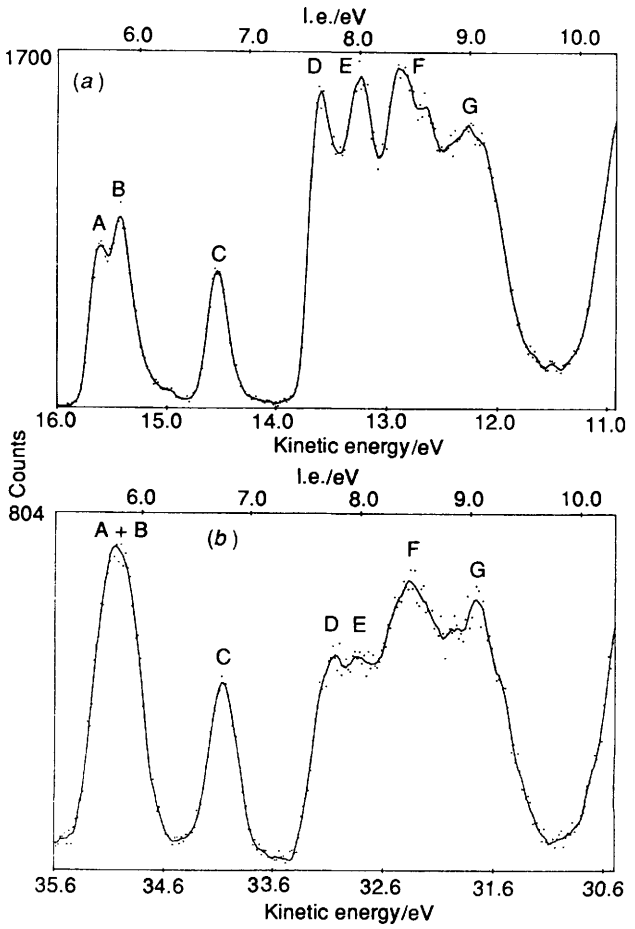

Figure 8. He I (*a*) and He II (*b*) p.e. spectra of $[Mo_2(\eta\text{-}C_5H_4Pr^i)_2(\mu\text{-}SMe)_4]$

of bands A—C on passing from He I to He II ionising radiation supports the assignment of these bands as arising from metal-based orbitals.[16] The bands D—G lying at higher ionisation energies show varying degrees of decrease in intensity in the He II spectrum compared to the He I spectrum. Therefore, the orbitals out of which ionisation has occurred are probably ligand-based. The bands D and E show the largest decrease in relative intensity and are assigned as arising from predominantly sulphur-based orbitals. Band F is in the expected region for ionisations arising from the η-cyclopentadienyl ring π orbitals,[16] and band G is assigned to electrons, which although largely localised on sulphur, have appreciably more bonding character than those giving rise to bands D and E. The p.e. spectra of compound (**4**) are largely consistent with the frontier-level ordering computed using extended-Hückel procedures for the model complex $[Mo_2(cp)_2(\mu\text{-}SH)_4]$.[6,7]

Although both formally $(Mo^{III})_2$ dimers, the μ-thiolato compound $[Mo_2(\eta\text{-}C_5H_4Pr^i)_2(\mu\text{-}SMe)_4]$ is substantially more electron-rich than the μ-halide analogue, (**3**). Assuming Koopmans' theorem, the p.e. data suggest that in the model complexes $[Mo_2(cp)_2(\mu\text{-}X)_4]$ (X = Cl or SH) the extended-Hückel calculations place the Mo–Mo σ orbital too close in energy to the δ/δ* orbitals. In addition, the bandwidths for ionisation from the σ, δ, and δ* orbitals in (**3**) and (**4**) are all similar. A narrow bandwidth is certainly to be expected for the δ interactions since, at a relatively long metal–metal separation, little effective metal–metal δ bonding or antibonding is anticipated. From the earlier discussion, one might also expect a narrow σ ionisation because of valence shell–outer core repulsion. However, the

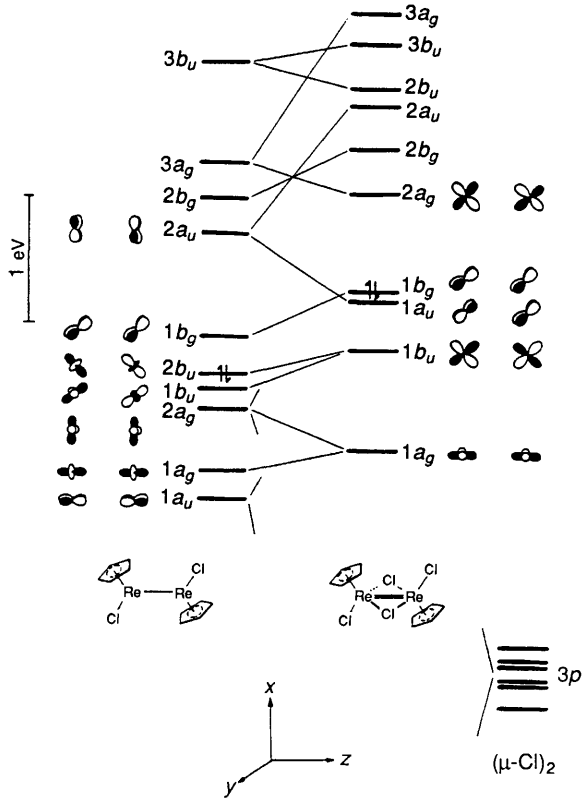

Figure 9. Interaction diagram for $[Re_2(cp)_2Cl_2(\mu\text{-}Cl)_2]$

importance of this effect at longer metal–metal separations is unclear, and another way to rationalise the relatively narrow width of the σ ionisation is to recognise that a significant increase in the Mo–Mo distance in the ^2A_g $[(\sigma)^1(\delta^*)^2(\delta)^2]$ ion state would cost heavily in terms of interligand repulsions in the $(\mu\text{-}X)_4$ bridge (see below). In other words, it is not known how flexible the $Mo_2(\mu\text{-}X)_4$ unit is, and rigidity in this unit could result in a narrow bandwidth for the σ ionisation.

A comparison of the δ/δ^* separations indicated by the p.e. spectra for $[Mo_2(\eta\text{-}C_5H_4Me)_2(\mu\text{-}Br)_4]$ (observed separation 0.5 eV) and $[Mo_2(\eta\text{-}C_5H_4Pr^i)_2(\mu\text{-}SMe)_4]$ (separation < 0.1 eV) supports the predicted trend of decreasing δ/δ^* separation with co-ordination of hydrocarbyl groups to the bridging ligands.[6,7] The expectation that the ligand-based lone-pair ($1b_g$) should fall in energy with co-ordination of substituents to the bridging ligands may also be supported by the p.e. data. Note that these two conclusions require that the relative level ordering of $[Mo_2(\eta\text{-}C_5H_4Me)_2(\mu\text{-}Br)_4]$ is a reasonable model for that of $[Mo_2(\eta\text{-}C_5H_4Pr^i)_2(\mu\text{-}S)_4]$.

It may be noted that the complex $[V_2(\eta\text{-}C_5Me_4Et)_2(\mu\text{-}Br)_4]$,[33] like the apparently related μ-thiolato species $[V_2(cp)_2(\mu\text{-}SR)_4]$ (*e.g.*, R = Me or Ph),[34] exhibits residual paramagnetism at room temperature. In these complexes the V–V interaction may be interpreted as comprising a V–V σ bond and a $(\delta^*)^1(\delta)^1$ triplet component, the 3*d* orbitals of vanadium being less diffuse than the 4*d* and 5*d* valence orbitals of its heavier congeners.

Type (**I**) *species: Extended-Hückel Molecular-orbital Study of* $[Re_2(cp)_2(Cl_2\mu\text{-}Cl)_2]$.—We turn now to the last structural type to be considered. The hypothetical type (**I**) complex $[Re_2(cp)_2Cl_2(\mu\text{-}Cl)_2]$ is based on the structurally characterised homologue $[Re_2(\eta\text{-}C_5Me_4Et)_2Cl_2(\mu\text{-}Cl)_2]$ idealised to C_{2h} symmetry.[8] The calculations described below apply only to type (**I**) species containing a metal–metal bond. The case of type (**I**) species that do not possess a metal–metal bond is discussed later in this paper. Detailed analyses of the molecular orbitals of the related species $[Re_2(cp)_2O_2(\mu\text{-}O)_2]$, $[Mo_2(cp)_2S_2(\mu\text{-}S)_2]$, and $[Mo_2(cp)_2H_2(\mu\text{-}H)_2]$,[25] and of the fragment $Re_2(cp)_2H_2$,[11] have been described previously.

Figure 9 shows the assembly of a compound orbital diagram for $[Re_2(cp)_2Cl_2(\mu\text{-}Cl)_2]$ from the fragments $Re_2(cp)_2Cl_2$ and $(\mu\text{-}Cl)_2$. The orbitals of the $Re_2(cp)_2Cl_2$ fragment (at left in Figure 9) are related to those of $[W_2(cp)_2Cl_4]$ described above. The principal effects of replacing two terminal Cl ligands lying above and below the *xz* plane by one Cl ligand contained in the *xz* plane are readily traced. The $\pi(yz)$ ($1a_u$) orbital of $Re_2(cp)_2Cl_2$ drops down in energy since the terminal Cl ligand is now contained within one of its nodal planes. In contrast, the metal $\pi(xz)$ orbital is directed towards this ligand and is pushed up in energy where it mixes with the metal σ^* and $\delta^*(x^2 - y^2)$ combinations to form the hybrid orbitals $1b_u$, $2b_u$, and $3b_u$. Just as the $\pi(yz)$ orbital is stabilized, so are the $\delta(xy)$ and $\pi^*(yz)$ levels which also mix and give rise to the hybrids $1b_g$ and $2b_g$.

The symmetry-adapted combinations of the six 3*p* orbitals of the $(\mu\text{-}Cl)_2$ fragment transform as $a_g + a_u + 2b_g + 2b_u$ under the C_{2h} symmetry of the complex, and the ten metal-based orbitals of the metal fragment transform as $3a_g + 2a_u + 2b_g + 3b_u$. Hence four $Re_2(cp)_2Cl_2$ fragment molecular orbitals (two a_g, one a_u, and one b_u) should be left without partners and thus remain non-bonding with respect to $Re_2(cp)_2Cl_2/(\mu\text{-}Cl)_2$ interactions.

At centre in Figure 9 is shown the resultant molecular-orbital diagram for $[Re_2(cp)_2Cl_2(\mu\text{-}Cl)_2]$. Introduction of the bridging ligands gives a general destabilisation of all the metal-based orbitals, although the largest effect is on the $\pi/\pi^*(yz)$ and $\delta/\delta^*(x^2 - y^2)$ combinations which form the basis of the σ framework of the $Re_2(\mu\text{-}Cl)_2$ bridge, combining with the in- and out-of-phase pairwise combinations of the μ-Cl p_z and p_y atomic orbitals.

Of the four occupied metal-based orbitals ($1a_g$ to $1b_g$), the $1a_g$ is $\sigma/\delta(x^2 - y^2)$ in character, $1b_u$ is essentially pure $\pi(xz)$, and the nearly isoenergetic $1a_u$ and $1b_u$ levels are $\delta^*(xy)/\pi(yz)$ and $\delta(xy)/\pi^*(yz)$ hybrids respectively. Contour diagrams of the $1a_g$, $1b_u$, $1a_u$, and $1b_g$ orbital wavefunctions are shown in Figure 10.

There is a modest computed energy separation between the $1b_g$ (h.o.m.o. for a d^4–d^4 dimer) and $2a_g$ [$\pi^*(xz)$, l.u.m.o. for a d^4–d^4 dimer] levels indicating that this is not an unreasonable model for a compound with the present electron count. The orbital occupancy indicates a formal net metal–metal double bond as anticipated from simple electron-counting procedures. Molecular-orbital calculations for the related complexes $[Mo_2(cp)_2X_2(\mu\text{-}X)_2]$ (X = O,[25] S,[7,25] or NH[35]) showed that the three orbitals $1b_u$, $1a_u$, and $1b_g$ are pushed up high in energy due to strong π donation from the terminal and bridging X ligands and, therefore, these complexes may only support a d^1–d^1 electron count. However, since Cl is only a poor π donor, this block ($1b_u$ to $1b_g$) of π-acceptor orbitals is only destabilised to a small extent and thus available for housing up to six more metal-based electrons. No p.e. data are available to corroborate this analysis.

Attempted Rationalisation of Structural type: Bridged or Non-bridged?—In the general class of compound $[\{M(\eta\text{-}C_5R_5)X_2\}_2]$, the metal *d* orbitals are expected to be contracted because of the electronegative nature of the halide ligands and the poor π-donor ability of the halide and cyclopentadienyl moieties, an effect which is nicely illustrated by comparison of the p.e. spectra of $[Mo_2(\eta\text{-}C_5H_4Me)_2(\mu\text{-}Br)_4]$ and $[Mo_2(\eta\text{-}C_5H_4Pr^i)_2(\mu\text{-}SMe)_4]$ (Figures 7 and 8). Within the series $[\{M(\eta\text{-}C_5R_5)X_2\}_2]$ the extent of orbital contraction for a given M will be fine-tuned by the precise identity of X and R, but will depend principally upon the position of M in the transition series. The

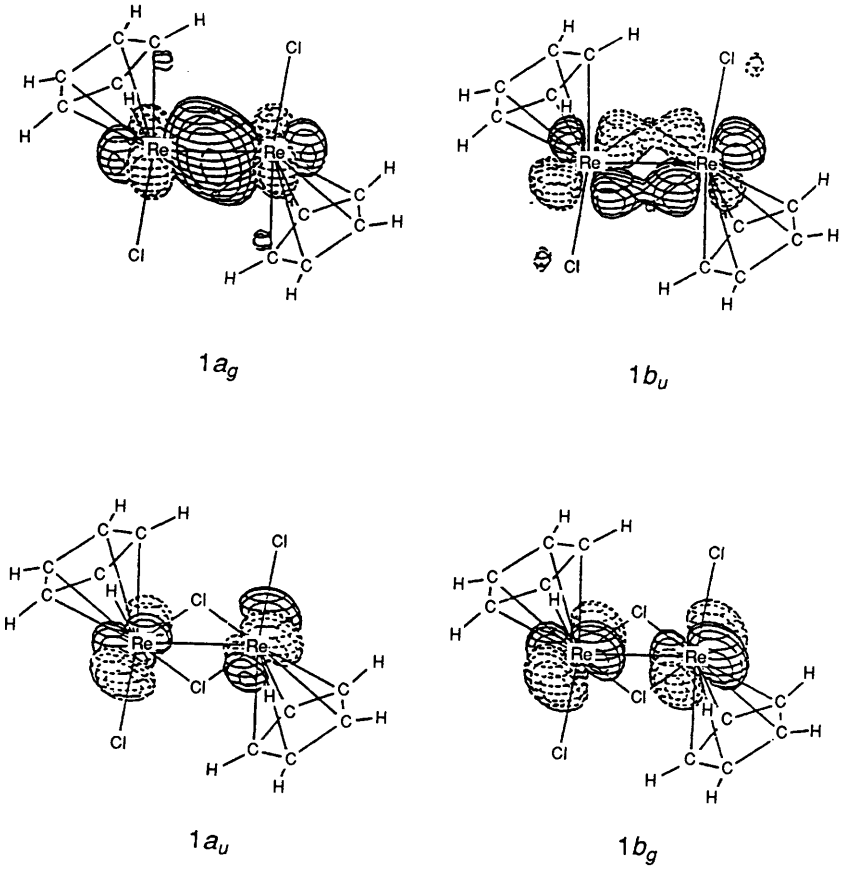

Figure 10. Contour diagrams of the $1a_g$, $1b_u$, $1a_u$, and $1b_g$ orbital wavefunctions of $[Re_2(cp)_2Cl_2(\mu\text{-}Cl)_2]$

Table 8. Comparison of Mo–Mo overlap populations for type (I)—(III) geometries

Complex[a]	Type	Overlap population[b]
$[Mo_2(cp)_2Cl_2(\mu\text{-}Cl)_2]$	(I)	0.387
$[Mo_2(cp)_2(\mu\text{-}Cl)_4]$	(II)	0.160
$[Mo_2(cp)_2Cl_4]$	(III)	0.773

[a] For all complexes Mo–Mo 2.50, Mo–Cl 2.40 Å. [b] Total computed Mo–Mo overlap population at given Mo–Mo distance.

Table 9. Comparison of metal–metal overlap populations for type (III) complexes

Complex[a]	Overlap population[b]
$[Mo_2(cp)_2Cl_4]$	0.773
$[Mo'_2(cp)_2Cl_4]$[c]	0.771
$[W_2(cp)_2Cl_4]$	0.889
$[W_2(cp)_2Cl_4]^{2-}$	0.956
$[Re_2(cp)_2Cl_4]$	0.687
$[Re'_2(cp)_2Cl_4]$[d]	0.823

[a] For all complexes: M–M 2.50, M–Cl = 2.40 Å; M–M–Cl = 106°. [b] Total computed metal–metal overlap population. [c] Using tungsten H_{ii} values and molybdenum exponents. [d] Using tungsten H_{ii} values and rhenium exponents.

identity of M will also control the number of electrons available for metal–metal bonding.

Table 8 lists computed total Mo–Mo overlap populations for hypothetical type (I)—(III) structures at a constant Mo–Mo separation. These data suggest that metal–metal bonding becomes of increasing importance in the order (II) < (I) < (III). It is clear that for a type (III) structure to be preferred to the alternative halide-bridged isomers [(I) or (II)] specific requirements of metal–metal overlap and *d*-electron count must be met since metal–metal interactions dominate at the expense of the formation of metal–halogen bonds. In practice, the type (III) structure has only been observed for M = W and X = Cl or Br. As one moves up, to the right, or to the left of W in the transition series then a different structural type is encountered.

For tantalum the 5*d* atomic orbitals are expected to be slightly less contracted than for tungsten, but for the hypothetical type (III) complex $[Ta_2(\eta\text{-}C_5R_5)_2Cl_4]$ only two electrons from each Ta atom are available for metal–metal bonding giving a very small h.o.m.o.–l.u.m.o. separation and also a substantially weaker metal–metal bond since there are only four metal electrons engaged in metal–metal bonding. A type (III) d^2–d^2 dimer would be expected to be Jahn–Teller unstable and in reality $[Ta_2(\eta\text{-}C_5Me_5)_2(\mu\text{-}Br)_4]$ adopts a quadruply bridged type (II) geometry. To date there are no compounds known to contain an unsupported metal–metal double bond.

For M = Mo or Re there is apparently a satisfactory *d*-electron count and therefore different factors are at work in inhibiting the formation of a type (III) structure for these derivatives. For the hypothetical type (III) species $[M_2(cp)_2Cl_4]$ (M = Mo or Re) the metal–metal interactions may be described as $(\sigma)^2(\pi)^4$ and $(\sigma)^2(\pi)^4(\delta)^2$ respectively; $[Mo_2(cp)_2Cl_4]$ is valence isoelectronic with $[W_2(cp)_2Cl_4]$, and $[Re_2(cp)_2Cl_4]$ is strictly isoelectronic with $[W_2(cp)_2Cl_4]^{2-}$. Table 9 presents computed total metal–metal overlap populations for a number of type (III) complexes at constant geometry. For the complexes $[M'_2(cp)_2Cl_4]$ (M' = Mo' or Re') the 5*d* H_{ii} values for W were used but the exponents of Mo and Re were retained.

The computed overlap populations reflect qualitative expectations: the 4*d* orbitals of Mo and the 5*d* orbitals of Re are less diffuse than the 5*d* orbitals of W affording diminished metal–metal bonding (as judged from the overlap populations). The results clearly suggest that there exists a very delicate balance between the optimisation of metal–metal or metal–ligand bonding in the congeneric pair $[\{M(\eta\text{-}C_5H_4R)X_2\}_2]$ (M = Mo or W, X = Cl or Br).

On passing from W to Re two different and opposing effects on the metal–metal bonding are encountered. The increased bonding between the two metal atoms that results from population of the $\delta(x^2 - y^2)$ $(2a_g)$ orbital {as indicated by the increase in W–W overlap population for $[W_2(cp)_2Cl_4]^{2-}$} is countered by a contraction of the 5*d* orbitals of Re compared to those of W. Since the complex $[Re_2(\eta\text{-}C_5Me_4Et)_2Cl_2(\mu\text{-}Cl)_2]$ adopts a type (**I**) structure rather than the alternative quadruply bonded type (**III**) alternative, orbital contraction is probably the more important effect (the δ component of a metal–metal multiple bond is generally accepted to be only weakly bonding compared to the σ and π components).

There is a second factor to consider here, namely the magnitude of the calculated h.o.m.o. – l.u.m.o. gap for the alternative structures for the *d*-electron count under consideration. For a d^4–d^4 dimer the type (**III**) structure has a small h.o.m.o. – l.u.m.o. gap compared with that of the type (**I**) alternative, and for a small h.o.m.o. – l.u.m.o. gap a high-spin complex or second-order Jahn–Teller distortion to another geometry becomes more likely. A similar argument was used by Hoffmann and co-workers[36] to explain the semi-bridging carbonyls in the $[M_2(cp)_2(CO)_4]$ (M = Cr or Mo) dimers.

Finally, it must be stressed that, *a priori*, these results could not be used to *predict* that the derivatives of Mo and Re would not adopt a type (**III**) geometry. They can, however, be used to help *rationalise* the observed structures by underlining the important factors which promote a type (**III**) geometry above a type (**I**) or (**II**) geometry.

Two or Four Halide Bridges?—In this section the factors deciding between a type (**I**) or (**II**) structure are sought out. Type (**I**) structures are known both for compounds containing metal–metal bonds, and for compounds in which no metal–metal bond exists. In contrast, type (**II**) structures are only known for metal–metal bonded species. First we shall consider complexes without a direct metal–metal bond.

For the purposes of this discussion a complex is defined as lacking a metal–metal bond when the metal–metal separation exceeds the sum of the covalent radii of the metal atoms. Suitable models for the metal centres in type (**I**) and (**II**) structures which contain no significant metal–metal interactions are the mononuclear complexes $[M(cp)X_3]^-$ and $[M(cp)X_4]^{2-}$ respectively. For $[M(cp)X_3]^-$ there are three low-energy metal-based orbitals, and for $[M(cp)X_4]^{2-}$ there are two. In principle, a metal–metal non-bonded type (**I**) complex can accommodate Group 3—9 transition metals. A metal–metal non-bonded type (**II**) complex can accommodate Group 3—7 transition metals. As far as data are available, however, only the type (**I**) structure is found for metal–metal non-bonded $[\{M(\eta\text{-}C_5R_5)X_2\}_2]$ complexes.

This feature can be traced to the geometrical requirements of a large metal–metal separation in complexes which do not contain a metal–metal bond. For a ligand-bridged complex, extending the M–M distance without increasing the M–X distance leads to a decrease in the X–M–X angle. These geometrical changes have drastic consequences for a type (**II**) structure since substantial (μ-X)–(μ-X) repulsions are turned on as the M–M distance increases. Thus increasing the Mo–Mo distance in $[Mo_2(cp)_2(\mu\text{-}Cl)_4]$ from 2.60 to 3.10 Å leads to a *ca.* 1 eV destabilisation of the $1b_g$ (chlorine-based lone-pair) orbital. The largest repulsions (as judged from overlap populations) are between mutually *cis* μ-Cl ligands, while only a small destabilisation is found for the μ-Cl ligands that are mutually *trans*. For a type (**I**) structure a much smaller destabilisation of the bridging ligands is found as the M–M separation increases.

A detailed description of the variation of the energy levels of the related hypothetical complex $[Mo_2(cp)_2(\mu\text{-}S)_4]$ with a change in Mo–Mo separation from 2.73 to 3.92 Å was published while this work was in progress, and supports the views presented here.[7] For $[Mo_2(cp)_2(\mu\text{-}S)_4]$, a geometry with a short metal–metal bond and long S • • • S separation is preferred.

The compound $[Ru_2(\eta\text{-}C_5Me_5)_2Cl_2(\mu\text{-}Cl)_2]$[37] possesses a non-metal–metal bonded type (**I**) geometry. According to formal electron-counting procedures, this compound might be expected to possess a metal–metal single bond between the two 17-valence-electron fragments. In practice, it is paramagnetic with a long Ru–Ru separation and $\mu_{eff.} = 1.89$ per ruthenium centre, a typical value for a low-spin ruthenium(III) complex. An explanation of the absence of a metal–metal bond can be gathered from a consideration of the interaction diagram for $[Re_2(cp)_2Cl_2(\mu\text{-}Cl)_2]$ given in Figure 9. For a d^5–d^5 dimer the $2a_g$ orbital (both M–M and M–Cl antibonding) must be filled. This orbital is relatively high in energy and leaves the net-metal–metal bonding interaction as $1a_g$, an orbital that contains significant δ character and is only weakly metal–metal bonding. Thus the required orbital occupancy, together with the relatively late position of ruthenium in the transition series, accounts for the absence of metal–metal bonding in this complex.

We turn now to the structural preferences of metal–metal bonded $[\{M(\eta\text{-}C_5R_5)X_2\}_2]$ complexes (the special case of M = W was discussed above). It is necessary to compare the level orderings for the two ligand-bridged structural alternatives within the same ligand framework and for the same metal atom. Figure 11 shows a correlation diagram for the symmetry-allowed opening-up process $[Mo_2(cp)_2(\mu\text{-}Cl)_4] \longrightarrow [Mo_2(cp)_2Cl_2(\mu\text{-}Cl)_2]$ at constant Mo–Mo and Mo–Cl bond lengths. Other workers have obtained similar correlation diagrams from extended-Hückel molecular-orbital calculations for the related $[Mo_2(cp)_2(\mu\text{-}S)_4] \longrightarrow [Mo_2(cp)_2S_2(\mu\text{-}S)_2]$ system.[6]

The μ-sulphido complexes have only two electrons to place in the metal–metal bonding manifold since each replacement of Cl

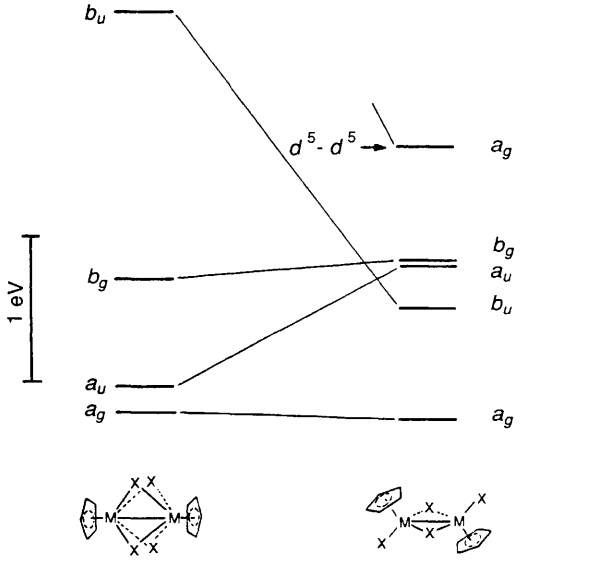

Figure 11. Correlation diagram for the opening of a quadruply bridged dimer to a doubly bridged dimer

by S amounts to a one-electron oxidation of the dimetal centre. The preference of the sulphido-supported dimers for a doubly- rather than quadruply-bridged complex has been attributed to (*i*) relief of a very small (< 0.1 eV) computed h.o.m.o. – l.u.m.o. gap in the tetrabridged species[6] or (*ii*) to removal of steric crowding in the $Mo_2(\mu\text{-}S)_4$ core.[7,25] As discussed earlier, the σ–δ^* energy separations in $[Mo_2(\eta\text{-}C_5R_5)_2(\mu\text{-}X)_4]$ (X = halide, S, or SR) compounds may have been significantly underestimated by the extended-Hückel calculations, and so arguments based on a near-degeneracy of the σ and δ^* levels should be treated with caution and, accordingly, more weight placed on arguments concerning repulsions within the bridge. However, correlations between the h.o.m.o. – l.u.m.o. gap and stable conformations have been noted previously in similar systems.[25] Within this constraint also a d^1–d^1 dimer would favour a type (**I**) over a type (**II**) geometry.

Some workers[6] have suggested that adding more electrons to the metal–metal manifold of $[Mo_2(cp)_2(\mu\text{-}S)_4]$ would favour (on metal-orbital energetics) a quadruply bridged structure over a doubly bridged one, and have modelled such a process by replacement of $(\mu\text{-}S)_2$ or $(\mu\text{-}S)_4$ by $(\mu\text{-}SH)_2$ or $(\mu\text{-}SH)_4$ respectively. Although the observation of quadruply bridged structures such as $[Mo_2(\eta\text{-}C_5R_5)_2(\mu\text{-}SR')_4]$ and $[Mo_2(\eta\text{-}C_5R_5)_2(\mu\text{-}SR')_2(\mu\text{-}S)_2]$ appears to confirm this hypothesis, it does not necessarily require that the driving force is to be found in the preferences of the metal-based orbitals alone. Co-ordination of alkyl groups to the sulphur ligands would lower the lone pair–lone pair non-bonding interactions between the bridging sulphur ligands.[25]

The halide-supported $[\{M(\eta\text{-}C_5R_5)X_2\}_2]$ series allows the possibility of probing the importance of the *d*-electron count without making substitutions at the bridging ligands. The correlation diagram for the opening-up process $[Mo_2(cp)_2(\mu\text{-}Cl)_4] \longrightarrow [Mo_2(cp)_2Cl_2(\mu\text{-}Cl)_2]$ suggests that for a d^1–d^1 dimer there is little preference for either structure in terms of valence-orbital energetics. The type (**I**) structure, however, may offer a larger h.o.m.o. – l.u.m.o. gap for a d^1–d^1 dimer, and also lowers the interligand repulsion in the $(\mu\text{-}Cl)_x$ bridge. Unfortunately, at this time, there are no structurally characterised Group 4 (d^1–d^1) $[\{M(\eta\text{-}C_5R_5)X_2\}_2]$ species with which to test this hypothesis. Presumably, should such a species be structurally characterised, it would feature a type (**I**) structure.

In contrast, a d^2–d^2 electron count would favour a closed [type (**II**)] structure based on metal-orbital energetics. The same reasoning can be applied to a d^3–d^3 dimer where a type (**I**) structure now has a near-degeneracy of the h.o.m.o. and l.u.m.o., but the quadruply bridged type (**II**) isomer has a stable 18-valence-electron count and a substantial h.o.m.o. – l.u.m.o. gap. That the type (**II**) structure persists even for the (presumably) more sterically congested $[M_2(\eta\text{-}C_5R_5)_2(\mu\text{-}Br)_4]$ (M = Mo or Ta) systems lends further weight to the implied importance of the *d*-electron count in setting the geometrical preferences in the d^2–d^2 and d^3–d^3 $[\{M(\eta\text{-}C_5R_5)X_2\}_2]$ dimers. Finally note that Figure 11 also shows the electronic driving force for the type (**I**) structure favoured for M = Re (d^4–d^4).

Conclusion

The computational and spectroscopic results described above successfully account for the geometrical preferences of species of the general formula $[\{M(\eta\text{-}C_5R_5)X_2\}_2]$ (X = halogen) and complement those reported by previous workers for the related species $[Mo_2(cp)_2(\mu\text{-}SH)_4]$ and $[Mo_2(cp)_2X_2(\mu\text{-}X)_2]$ (X = O, S, or NH). In the studies undertaken here an understanding of the geometrical preferences was made more clear with the benefit of hindsight for the crystallographically characterised examples. As anticipated, the preferred structural type depends principally upon the *d*-electron count, but is also critically dependent on the radial extension of the *d* orbitals of the particular metal in question. This is most dramatically illustrated by considering the solid-state molecular structures of the Group 6 series $[Cr_2(cp)_2Cl_2(\mu\text{-}Cl)_2]$ [type (**I**), no metal–metal bond],[38] $[Mo_2(\eta\text{-}C_5H_4Pr^i)_2(\mu\text{-}Cl)_4]$ [type (**II**), Mo–Mo single bond],[2] and $[W_2(\eta\text{-}C_5H_4Pr^i)_2Cl_4]$ [type (**III**), W≡W triple bond].[1] Where the differences in metal–metal bonding between two structural alternatives do not uniquely define the preferred isomer, interligand repulsions within the bridge appear to select the observed geometry.

It would now appear very likely that the green, structurally uncharacterised diniobium species $[\{Nb(\eta\text{-}C_5Me_5)Cl_2\}_2]$ adopts a quadruply bridged type (**II**) structure rather than the type (**I**) alternative proposed previously.[39] Although this material has a slightly different chemical reactivity to its tantalum congener (*e.g.* the former does not oxidatively add H_2 across the metal–metal bond), these differences probably just reflect the greater ease of oxidation of third-row over second-row transition metals.

Acknowledgements

We thank the S.E.R.C. and British Petroleum plc for a C.A.S.E. award (to P. M.) and Dr. D. L. Clark for helpful discussion.

References

1 M. L. H. Green and P. Mountford, *J. Chem. Soc., Chem. Commun.*, 1989, 732.
2 P. D. Grebenik, M. L. H. Green, A. Izquierdo, V. S. B. Mtetwa, and C. K. Prout, *J. Chem. Soc., Dalton Trans.*, 1987, 9.
3 R. Hoffmann and W. N. Lipscomb, *J. Chem. Phys.*, 1962, **36**, 2179.
4 M. L. H. Green, J. D. Hubert, and P. Mountford, *J. Chem. Soc., Dalton Trans.*, in the press.
5 D. P. S. Rodgers, D. Phil. Thesis, Oxford, 1984.
6 D. L. DuBois, W. K. Miller, and M. Rakowski-DuBois, *J. Am. Chem. Soc.*, 1981, **103**, 3429.
7 W. Tremmel, R. Hoffmann, and E. D. Jemmis, *Inorg. Chem.*, 1989, **28**, 1213.
8 W. A. Herrmann, R. A. Fischer, and E. Herdtweck, *J. Organomet. Chem.*, 1987, **329**, C1.
9 R. Hoffmann, *J. Chem. Phys.*, 1963, **39**, 1397; R. H. Summerville and R. Hoffmann, *J. Am. Chem. Soc.*, 1976, **98**, 7240; A. Dedieu, T. A. Albright, and R. Hoffmann, *J. Am. Chem. Soc.*, 1979, **101**, 3141.
10 B. E. R. Schilling, R. Hoffmann, and D. L. Lichtenberger, *J. Am. Chem. Soc.*, 1979, **101**, 585; B. E. R. Schilling, R. Hoffmann, and J. W. Faller, *ibid.*, p. 592.
11 B. E. Bursten and R. J. Cayton, *Organometallics*, 1988, **7**, 1349.
12 J. L. Davidson, K. Davidson, W. E. Lindsell, N. W. Murrall, and A. J. Welch, *J. Chem. Soc., Dalton Trans.*, 1986, 1677.
13 B. E. Bursten, F. A. Cotton, J. C. Green, E. A. Seddon, and G. G. Stanley, *J. Am. Chem. Soc.*, 1980, **102**, 4579.
14 F. A. Cotton, G. G. Stanley, B. J. Kalbacher, J. C. Green, E. A. Seddon, and M. H. Chisholm, *Proc. Natl. Acad. Sci. USA*, 1977, **74**, 3109.
15 M. H. Chisholm, D. L. Clark, E. M. Kober, and W. G. Van Der Sluys, *Polyhedron*, 1987, **6**, 723.
16 J. C. Green, *Struct. Bonding (Berlin)*, 1981, **43**, 37.
17 G. M. Bancroft, E. Pellach, A. P. Sattelberger, and K. W. McLaughlin, *J. Chem. Soc., Chem. Commun.*, 1982, 752.
18 F. A. Cotton, J. L. Hubbard, D. L. Lichtenberger, and I. Shim, *J. Am. Chem. Soc.*, 1982, **104**, 679.
19 M. H. Chisholm, D. L. Clark, J. C. Huffman, W. G. Van Der Sluys, E. M. Kober, D. L. Lichtenberger, and B. E. Bursten, *J. Am. Chem. Soc.*, 1987, **109**, 6796.
20 A. W. Coleman, J. C. Green, A. J. Hayes, W. A. Seddon, D. R. Lloyd, and Y. Niwa, *J. Chem. Soc., Dalton Trans.*, 1979, 1057.
21 E. M. Kober and D. L. Lichtenberger, *J. Am. Chem. Soc.*, 1985, **107**, 7199.
22 B. J. Morris-Sherwood, C. B. Powell, and M. B. Hall, *J. Am. Chem. Soc.*, 1984, **106**, 4079.
23 M. L. H. Green and P. Mountford, *Organometallics*, 1990, **9**, 886.

24 M. H. Chisholm, M. J. Hampden-Smith, J. C. Huffman, J. D. Martin, K. A. Stahl, and K. G. Moodley, *Polyhedron*, 1988, **7**, 1991.
25 B. E. Bursten and R. H. Cayton, *Inorg. Chem.*, 1989, **28**, 2846.
26 J. Wachter, *J. Coord. Chem., Sect. B*, 1987, **15**, 219.
27 M. Elian, M. L. M. Chen, D. M. P. Mingos, and R. Hoffman, *Inorg. Chem.*, 1976, **15**, 1148.
28 J. A. M. Canich, F. A. Cotton, L. M. Daniels, and D. B. Lewis, *Inorg. Chem.*, 1987, **26**, 4046; F. A. Cotton, *Polyhedron*, 1987, **6**, 667.
29 L. Messerle, *Chem. Rev.*, 1988, **88**, 1229.
30 T. Koopmans, *Physica*, 1934, **1**, 104.
31 C. Ting, N. C. Baezinger, and L. Messerle, *J. Chem. Soc., Chem. Commun.*, 1988, 1133.
32 S. Evans, J. C. Green, A. F. Orchard, T. Saits, and D. W. Turner, *Chem. Phys. Lett.*, 1969, **4**, 361; P. A. Cox and A. F. Orchard, *ibid.*, 1970, **7**, 273.
33 L. Messerle, personal communication.
34 R. H. Holm, R. B. King, and F. G. A. Stone, *Inorg. Chem.*, 1963, **2**, 219.
35 M. L. H. Green, G. Hogarth, P. Konidaris, and P. Mountford, *J. Organomet. Chem.*, 1990, in the press; *J. Chem. Soc., Dalton Trans.*, in the press.
36 E. D. Jemmis, A. R. Pinhas, and R. Hoffmann, *J. Am. Chem. Soc.*, 1980, **102**, 2576.
37 U. Koelle and J. Kossakowski, *J. Organomet. Chem.*, 1989, **362**, 383.
38 F. H. Köhler, R. de Cao, K. Ackemann, and J. Sedlmair, *Z. Naturforsch., Teil B*, 1983, **38**, 1406.
39 P. A. Belmonte, F. G. N. Cloke, K. H. Theopold, and R. R. Schrock, *Inorg. Chem.*, 1984, **23**, 2365.

Received 22*nd June* 1990; *Paper* 0/02794D